Canadian Conference - Pacific Conference on Earthquake Engineering 2023
Vancouver, British Columbia
June 25th – June 30th, 2023

Influence of Different Design Factors on the Seismic Response of Coupled Composite Plate Shear Walls/Concrete Filled

Mohammad Froozanfar[1], Saber Moradi[2*] and Reza Kianoush[3]

[1]PhD Candidate, Department of Civil Engineering, Toronto Metropolitan University, Toronto, ON, Canada
[2]Associate Professor, Department of Civil Engineering, Toronto Metropolitan University, Toronto, ON, Canada
[3]Professor, Department of Civil Engineering, Toronto Metropolitan University, Toronto, ON, Canada
[*]s.moradi@torontomu.ca (Corresponding Author)

ABSTRACT

Composite plate shear wall/concrete filled (C-PSW/CF), also named "SpeedCore" system by the American Institute of Steel Construction (AISC), comprises two steel plates, tie bars, shear studs, and infilled concrete. These new seismic force-resisting systems have been recently adopted in ASCE 7-22 with the highest response modification coefficient. Past experimental and numerical studies have verified their high stiffness and strength, desired ductility, and energy dissipation. This paper develops high-fidelity finite element models for C-PSWs/CF and performs a sensitivity analysis of their cyclic response. A statistical "design of experiments" method is used to determine the design factor effects and interactions. Different geometric- and material-related design factors influencing the seismic response of the walls are considered and evaluated through sensitivity analysis. These factors include the aspect ratio of the coupling beams, the ratio of the coupling beams' thickness to the walls' thickness, the length, total thickness, and the walls' steel faceplate thickness, steel yield strength, and concrete compressive strength. The study determines influential factors on response parameters, such as stiffness, strength, and damage sequences. According to the results, the length of the wall and the ratio of the coupling beams' thickness to the walls' thickness are the most crucial factors affecting most responses.

Keywords: Composite plate shear wall/concrete filled (C-PSW/CF), SpeedCore, Coupled wall, Sensitivity analysis, Seismic behavior

INTRODUCTION

Seismic design standards suggest different lateral-force resisting systems for mid- to high-rise buildings, including reinforced concrete (RC) core walls [1]. Composite plate shear wall/concrete filled (C-PSW/CF), also named "SpeedCore" by the American Institute of Steel Construction (AISC), was recently adopted by the ASCE7-16 [2] (uncoupled configuration) and ASCE7-22 [3] (coupled configuration) as an alternative to RC core walls. C-PSW/CF comprises two steel plates, tie bars, shear studs, and infilled concrete [4]. Steel faceplates are the permanent formwork for the concrete, connected through the tie bars. Tie bars also prevent steel faceplates' local buckling, while shear studs provide a composite action between steel faceplates and the infilled concrete [4,5].

C-PSWs/CF have advantages over traditional RC core walls, as they eliminate construction requirements, such as concrete curing time, formwork, and rebars [4,5]. Hence, C-PSWs/CF reduce the construction time noticeably [5]. The 58-story Rainier Square Tower, Seattle, U.S., is the first and tallest project utilizing this innovative system with a 40% faster construction than the RC core [1], followed by the under-construction 19-story 200 Park Avenue, San Jose.

Past experimental and numerical studies have verified high stiffness and strength, desired ductility, and energy dissipation of C-PSWs/CF [6-9]. Coupled C-PSW/CF is preferred over uncoupled configuration in higher buildings and for higher demands. A comprehensive numerical study based on the FEMA-P695 has determined a response modification coefficient of 8, an over-strength factor of 2.5, and a deflection amplification factor of 5.5 for the CC-PSWs/CF [10]. Further, CC-PSW/CF has the highest response modification coefficient among all lateral-force resisting systems in ASCE7-22 [3]. Although previous experimental and numerical studies have evaluated the behavior of C-PSWs/CF, the coupled configuration has received less attention, with a few studies (e.g., [1, 10, 11]). This paper has tried to provide a more profound knowledge of the response of SpeedCore systems.

MOTIVATION AND OBJECTIVE OF THIS STUDY

CC-PSWs/CF comprise composite walls and coupling beams, and different design factors can affect the behavior and response of the system under lateral loading. Previous research has evaluated the system's behavior under non-linear static and cyclic analyses. However, cyclic analysis of the system with different design factors has not been investigated. In this paper, three-dimensional finite element models are developed and validated against previous experimental and numerical studies. A two-level fractional factorial design with seven factors is used for a statistical response sensitivity analysis. The selected design factors include walls and coupling beams geometry-related and material-related factors. Sixteen finite-element models of CC-PSW/CF are analyzed, and the cyclic force-displacement response of the models is investigated. This paper contributes to the comprehension of CC-PSWs/CF as one of the most reliable seismic-force resisting systems.

FINITE ELEMENT MODEL

Descriptions of the model

Three-dimensional finite element models are developed and analyzed via the general-purpose FEA program ABAQUS [12]. The PG-1B 8-story CC-PSW/CF model of a comprehensive report [13] to find the seismic design coefficients and factors for coupled composite plate shear walls/concrete filled (CC-PSW/CF) was selected as the basis of the numerical modeling. Table 1 shows the dimensional properties of the PG-1B model. The finite element model includes composite walls and coupling beams. The tie bars and shear studs are not modeled, and a tie constraint was developed between steel and concrete parts, as this study aimed to investigate factors related to the walls and coupling beams dimensions and materials. The steel and concrete material properties are shown in Table 2. Popovic's concrete material model with compressive strength (f_c') of 48.2 MPa was used for the infilled concrete.

All parts are modeled with C3D8R solid elements. Based on the reference report [13], the mesh density of 304.8 mm (12 in) showed good consistency with finer mesh sizes (6 in and 3 in). Hence, the concrete and steel parts of the walls have a 300 mm mesh size. For the coupling beams, a finer mesh of 150 mm was selected for both steel and concrete, as the coupling beams will act as the primary energy dissipation elements of the wall system. Each wall had 2574 and 3510 elements for the concrete and steel parts, respectively, and each coupling beam had 256 and 320 elements for the concrete and steel parts, respectively. The entire model was developed with 16776 elements (Fig. 1). Further, the walls' out-of-plane degrees of freedom are restrained (U3, UR1, and URR2). A 29-second dynamic implicit analysis was conducted with a 0.01 initial increment.

Table 1. Dimensional Properties of the PG-1B CC-PSW/CF Model.

Factors	Unit	Value
First story height	mm	5181.6
Upper stories height	mm	4267.2
Wall length	mm	3352.8
Total wall thickness	mm	609.6
Wall steel plate thickness	mm	14.3
Coupling beams length	mm	2438.4
Coupling beams dimensions	mm	609.6 × 609.6
Coupling beams steel thickness	mm	9.25 & 12.7

Table 2. Steel and Concrete Material Properties of the PG-1B CC-PSW/CF Model.

Steel			Concrete		
Properties	**Unit**	**Value**	**Properties**	**Unit**	**Value**
Young's modulus	MPa	2e5	Young's modulus	MPa	3.1702 e4
Poisson's ratio	-	0.3	Poisson's ratio	-	0.2
Mass density	Kg/m^3	7850	Mass density	Kg/m^3	2400
Yield stress	MPa	344.7	Compressive strength	MPa	48.2
Ultimate stress	MPa	448	Dilation angle	^{o}	40
Ultimate strain	mm/mm	0.15	Eccentricity	-	0.1
			F_{b0}/f_{c0}	-	1.2
			K	-	0.667
			Viscosity parameter	-	0.001

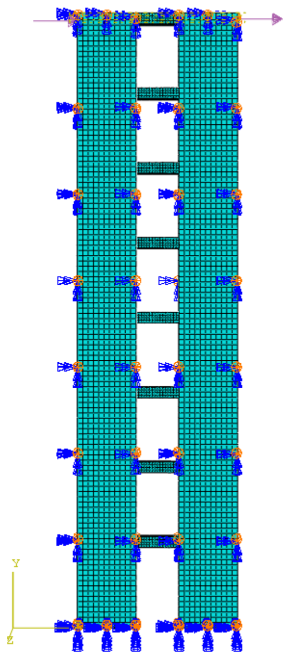

Figure 1. CC-PSW/CF mesh sizes and boundary conditions.

Validation of finite element analysis

Three-dimensional finite element models are validated against the PG-1B model of [13] and the uncoupled, single-story CW-42-55-10-T experimental and numerical model in [9]. Fig. 2 shows excellent consistency between the first mode shape of the PG-1B model and that of this paper's finite element model. Further, the maximum shear capacity of the PG-1B model is reported as 8015 KN (1802 kip), which is 3% less than the maximum base shear of this paper. Further, Fig. 3 shows acceptable consistency between the lateral force-displacement diagram of the CW-42-55-10-T model and the validated model.

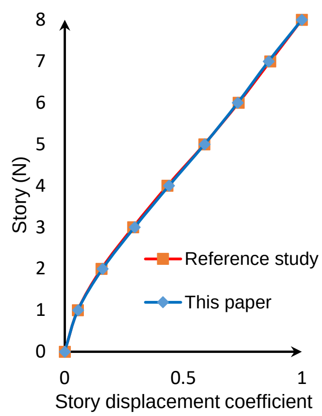

Figure 2. Comparison of the first modal shape from the PG-1B model and the validated model in this paper.

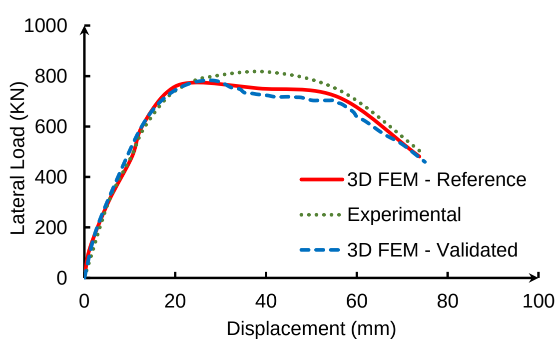

Figure 3. Lateral-force displacement diagram of the CW-42-55-10-T model and the response from the validated model.

SENSITIVITY ANALYSIS

Factors and their levels

The validated finite element model is used for the sensitivity analysis based on seven potentially influential design factors. Five geometry-related factors are the aspect ratio of the coupling beams (A), the ratio of the coupling beams' thickness to the walls' thickness (B), the length of the wall (C), the total thickness of the wall (D), and the walls' steel faceplate thickness (E). Further, two material-related design factors of steel yield strength (F) and concrete compressive strength (G) are included. Two levels, low (−) and high (+), are considered for each factor based on practical ranges for CC-PSWs/CF and the dimensions and materials of the validated model. For instance, the aspect ratio of the coupling beams is suggested to be from 3 to 5 in the literature [13]. Further, the coupling beams' thickness was selected to be lesser than or equal to the thickness of the walls. Table 3 lists the factors, their units, and low and high levels. In this study, the number of stories and the total height of the system is set constant. This was because the study aimed to investigate the effects of the seven parameters in the 8-story category.

Table 3. Design Factors and Levels Considered in the Sensitivity Analysis.

Factors	Symbol	Low level (−)	High level (+)	Units
The aspect ratio of the coupling beams	A	3	5	-
The ratio of the coupling beams' thickness to the walls' thickness	B	0.6	1	-
The length of the wall	C	2000	5000	mm
The total thickness of the wall	D	500	700	mm
The walls' steel faceplate thickness	E	8	20	mm
Steel yield strength	F	300	500	MPa
Concrete compressive strength	G	30	60	MPa

Design of experiments

The Design-Expert software [14] was utilized to conduct the two-level fractional factorial design. Seven factors related to the geometry and material of the CC-PSW/CF produce 128 (i.e., 2^7) cases or models – if a full-factorial design is conducted. In order to reduce computational efforts, a fraction (one-eighth) of the full-factorial design, called fractional factorial design, is considered in this study [15], and the number of models is reduced to 16 (i.e., 2^{7-3}). This design is suitable for screening. Since 16 models (listed in Table 4) are equivalent to a full-factorial design with four factors, and seven factors are considered in this study (Table 5), some generators are required to assign low or high levels to the three remaining factors.

A finite element analysis was conducted under cyclic loading based on the loading protocol of an experimental test [16] (Figs. 4 and 5). Twelve responses are recorded from each analysis. The responses are the initial stiffness (K_i), the corresponding lateral displacement and the onset of initial yielding of the coupling beams (δ_{yCB} and t_{yCB}), the corresponding lateral displacement and time of the first (δ_{phCB8} and t_{fhCB1}) and the last (δ_{phCB8} and t_{fhCB8}) plastic hinge at the coupling beams, the corresponding lateral displacement and time of the initial yielding at the walls (δ_{yW} and t_{yW}), and the maximum base shear (V_{max}), and the corresponding displacement and time (δ_{Vmax} and t_{Vmax}).

Table 4. The 2^{7-3} Fractional Factorial Design.

Model	A (-)	B (-)	C (mm)	D (mm)	E (mm)	F (MPa)	G (MPa)
1	5	1	2000	700	8	300	30
2	3	0.6	2000	700	8	500	60
3	5	0.6	5000	500	8	500	30
4	3	0.6	2000	500	8	300	30
5	5	1	5000	500	20	300	30
6	5	0.6	2000	700	20	500	30
7	3	1	5000	700	8	500	30
8	3	1	2000	500	20	500	30
9	3	1	5000	500	8	300	60
10	3	0.6	5000	500	20	500	60
11	5	1	5000	700	20	500	60
12	5	0.6	5000	700	8	300	60
13	5	0.6	2000	500	20	300	60
14	3	1	2000	700	20	300	60
15	3	0.6	5000	700	20	300	30
16	5	1	2000	500	8	500	60

Table 5. Design of Experiments Table and the Selected Design.

Design of experiments		**Number of factors**						
		2	3	4	5	6	7	8
Runs	4	2^{2}	2^{3-1}	-	-	-	-	-
	8	-	2^{3}	2^{4-1}	2^{5-2}	2^{6-3}	2^{7-4}	-
	16	-	-	2^{4}	2^{5-1}	2^{6-2}	2^{7-3}	2^{8-4}
	32	-	-	-	2^{5}	2^{6-1}	2^{7-2}	2^{8-3}

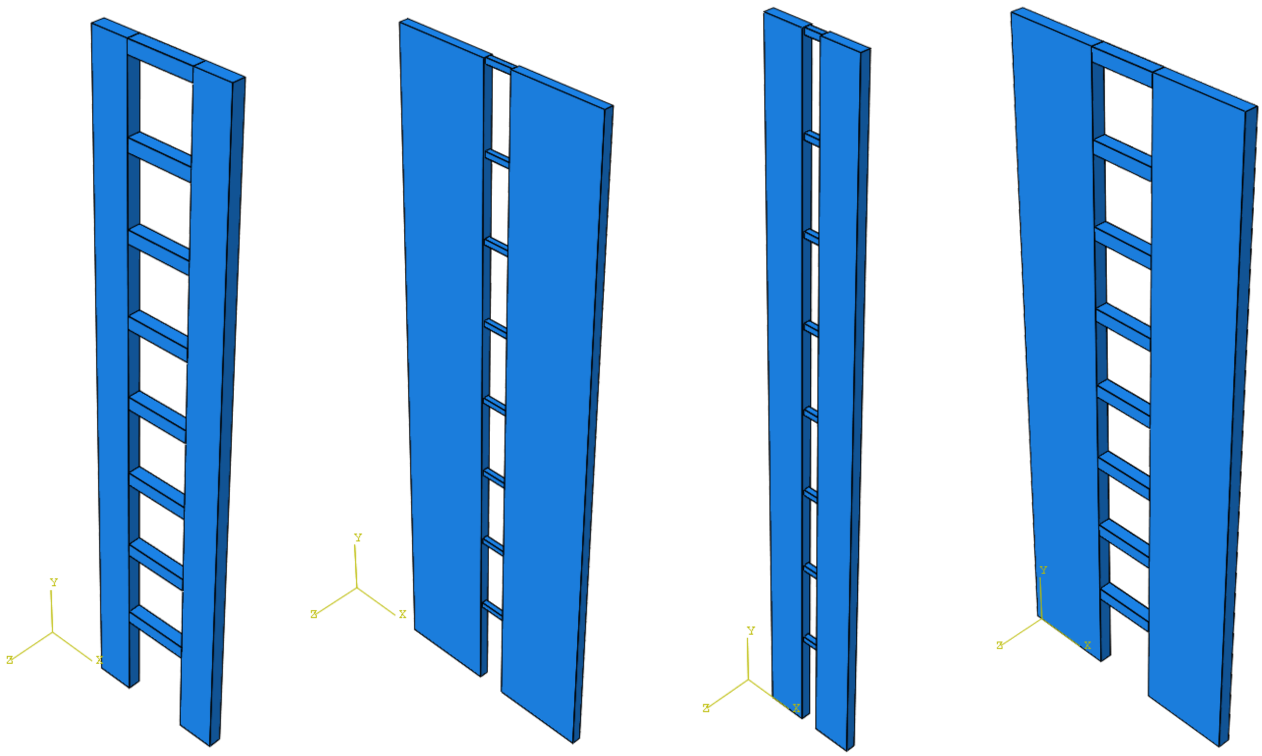

(a) *(b)* *(c)* *(d)*

Figure 4. Examples of the considered models: (a) model-1, (b) model-3, (c) model-4, (d) model-11.

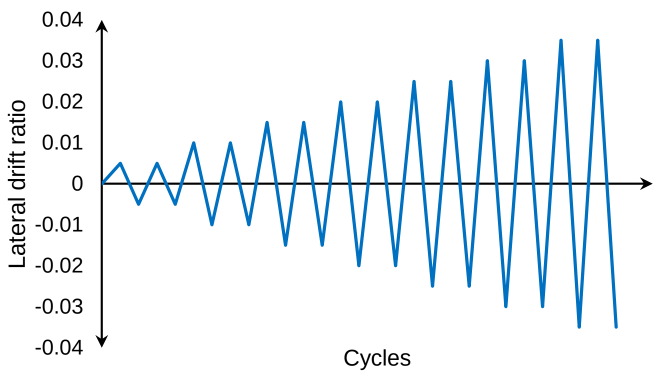

Figure 5. The cyclic load applied to the models.

RESULTS AND DISCUSSIONS

The force-displacement cyclic response and the visualization tools of stress and strain distributions of the models in all increments are monitored. Then, the values of the response parameters are recorded, as shown in Table 6. Figure 6 shows the force-displacement diagram of two models, 7 and 8.

Behavioral sequence

Full details of the behavioral sequences are shown in Table 6 and Fig. 7. Each model was run from 0 to 29s under dynamic implicit analysis. The capacity-based design of the CC-PSW/CF systems requires a sequence of events to ensure a desired behavior. As the lateral load increases, one of the coupling beams experiences yielding, followed by experiencing a plastic hinge, preferably a flexural hinge at the ends. The walls might have experienced the first yielding at this stage. The lateral load increases further until all coupling beams have developed plastic hinges at both ends. At this point, the walls must not have experienced a plastic hinge at the base to guarantee the "strong wall-weak coupling beam" design strategy. The lateral displacement increases until the walls experience a plastic hinge at the base, where the maximum demands exist. Some analyzed models do not follow this sequence as the capacity-based procedure is not applied. For instance, model 1 did not experience any flexural plastic hinge at the beams' end; instead, the walls experienced severe damage. Models 1, 7, and 11 experienced maximum shear capacity before the plastic hinge development at the end of all coupling beams. Moreover, for some models (e.g., 2, 4, 5, 9, 10, 12, 14, and 15), maximum shear capacity occurred with a time delay from developing the last flexural plastic hinge at the end of coupling beams, resulting in high ductility.

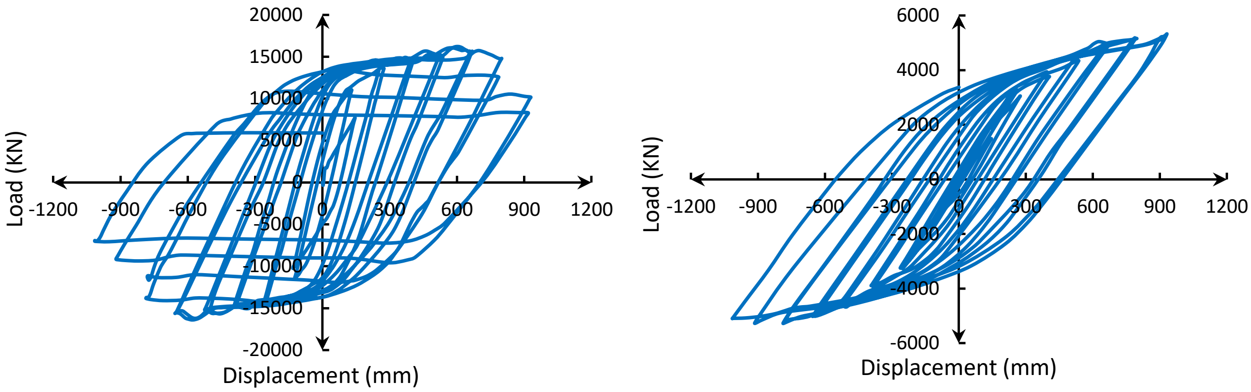

(a) *(b)*

Figure 6. Force-displacement diagrams: (a) model-7, (b) model-8.

Table 6. Design of Experiments Results.

Model	K_i (KN/mm)	δ_{yCB} (mm)	t_{yCB} (s)	δ_{fhCB1} (mm)	t_{fhCB1} (s)	δ_{fhCB8} (mm)	t_{fhCB8} (s)	δ_{yW} (mm)	t_{yW} (s)	V_{max} (KN)	δ_{Vmax} (mm)	t_{Vmax} (s)
1	32.8	139.1	4.59	×	×	×	×	121.7	1.87	3679	624.2	18.90
2	42.1	206.6	4.72	159.7	5.72	480.8	12.83	263.2	4.85	3440	883.3	25.91
3	134.9	61.2	0.34	121.3	0.68	415.6	8.99	216.3	4.73	7536	341.0	9.84
4	24.2	117.1	0.66	132.9	4.58	262.1	6.03	254.5	4.83	1829	928.3	24.97
5	183.6	53.2	0.30	105.5	0.60	266.5	6.01	155.0	4.62	12084	850.8	24.86
6	37.1	165.6	4.65	207.7	5.80	660.4	18.03	595.7	16.8	4251	1021	29*
7	331.0	137.6	1.98	258.6	4.82	×	×	137.6	1.98	16392	579.3	17.85
8	36.5	276.4	4.94	354.6	8.8	668.4	17.01	407.1	8.96	5314	931.5	25.00
9	268.9	64.8	0.36	113.2	0.63	217.8	4.74	106.1	0.59	7921	780.0	25.83
10	190.1	44.3	0.25	64.2	0.36	133.5	2.00	228.8	6.83	14729	827.9	25.86
11	289.3	116.4	0.66	225.7	4.76	537.6	13.99	240.6	4.79	21917	339.7	9.84
12	217.9	44.6	0.25	107.5	0.61	275.6	4.89	142.2	0.82	6992	716.7	21.86
13	27.7	57.1	0.33	142.7	0.83	254.2	7.98	350.9	8.81	2332	660.7	16.94
14	76.8	164.0	4.64	158.9	5.72	408.6	8.97	145.1	4.61	5849	871.6	26.90
15	334.4	46.3	0.26	55.0	0.31	133.6	2.98	133.1	4.58	13523	829.6	26.86
16	34.6	207.3	4.72	529.4	13.98	663.6	18.01	255.6	4.83	3337	916.8	25.97

× The phenomenon did not occur by the end of the analysis

* The model did not reach its maximum capacity by the end of the analysis

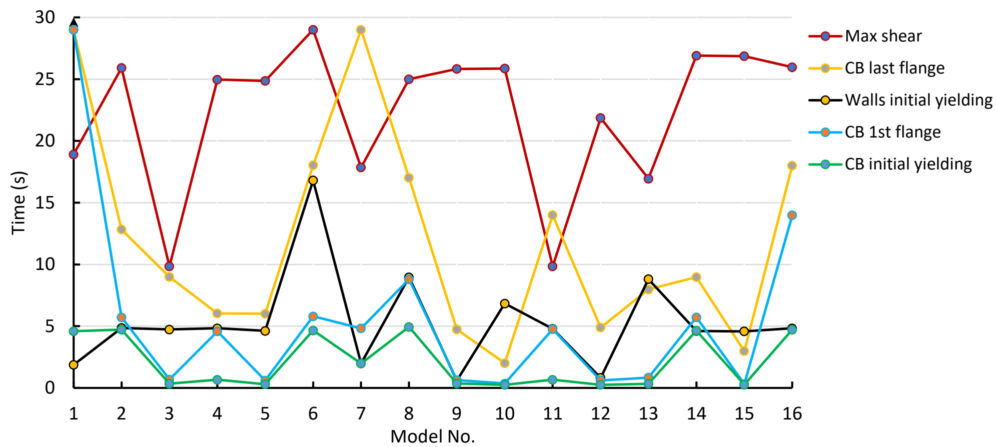

Figure 7. The sequence of behavioral patterns in the analyzed models.

Initial stiffness

A half-normal probability plot and Pareto chart are used to determine the most influential factors and interactions on the initial stiffness value (Fig. 8). Based on the results, the most significant factor is the length of the wall (C), with an 81.0% contribution percentage. The total thickness of the wall (D), the aspect ratio of the coupling beams (A), the interaction between the aspect ratio of the coupling beams and the concrete compressive strength (AG), the interaction between the aspect ratio of the coupling beams and the length of the wall (AC), and the ratio of the coupling beams' thickness to the walls' thickness (B) are other influential factors, with lower effects. The findings are also confirmed through the analysis of variance (ANOVA) using the Design-Expert software. In ANOVA, the significant factors have p-values of less than a defined significance level of 5%. All mentioned factors positively affect the responses, except A and AC.

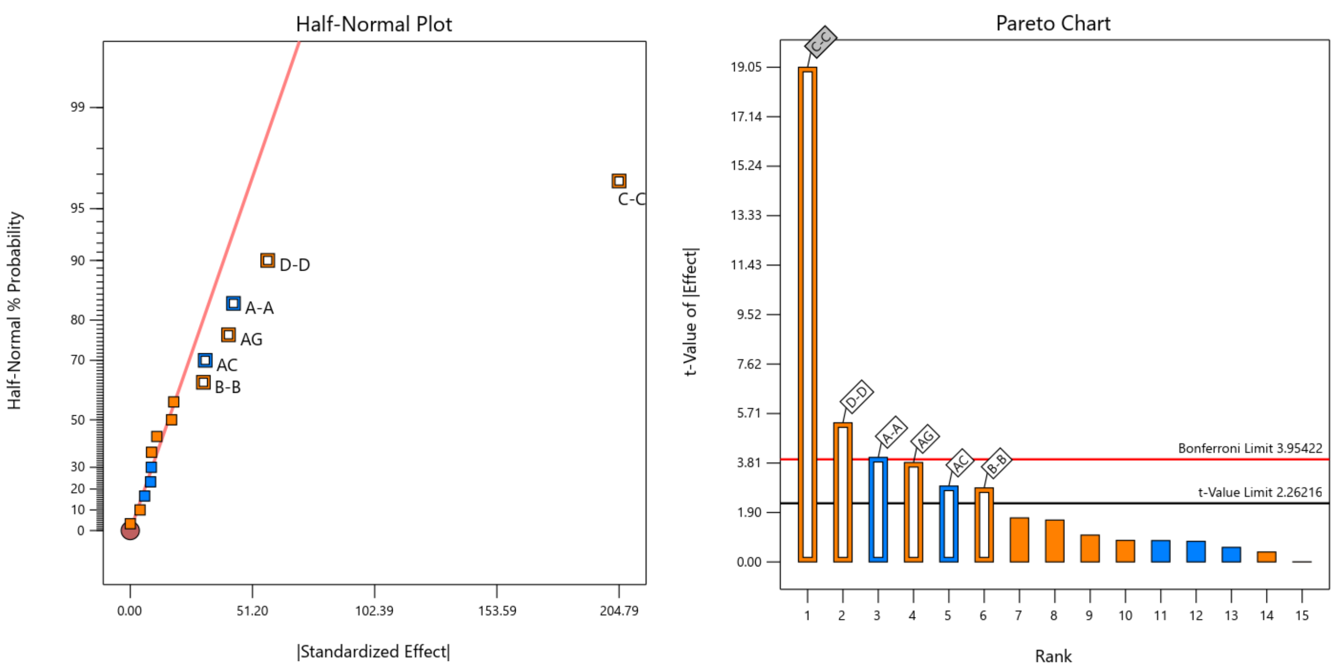

(a) *(b)*

Figure 8. Sensitivity analysis results for the initial stiffness: (a) half-normal probability plot, (b) Pareto chart.

Coupling beams' initial yielding

According to the results of the sensitivity analysis (Fig. 9), three factors, the length of the wall (C), steel yield strength (F), and the ratio of the coupling beams' thickness to the walls' thickness (B) are more influential on the coupling beams' initial yielding. Based on the time monitoring results, BD, AE, and AG interactions are also influential. The length of the wall factor had a 56.9% contribution and a standardized effect of −3.1. Factor C negatively affects the responses, while F, B, and D have positive effects.

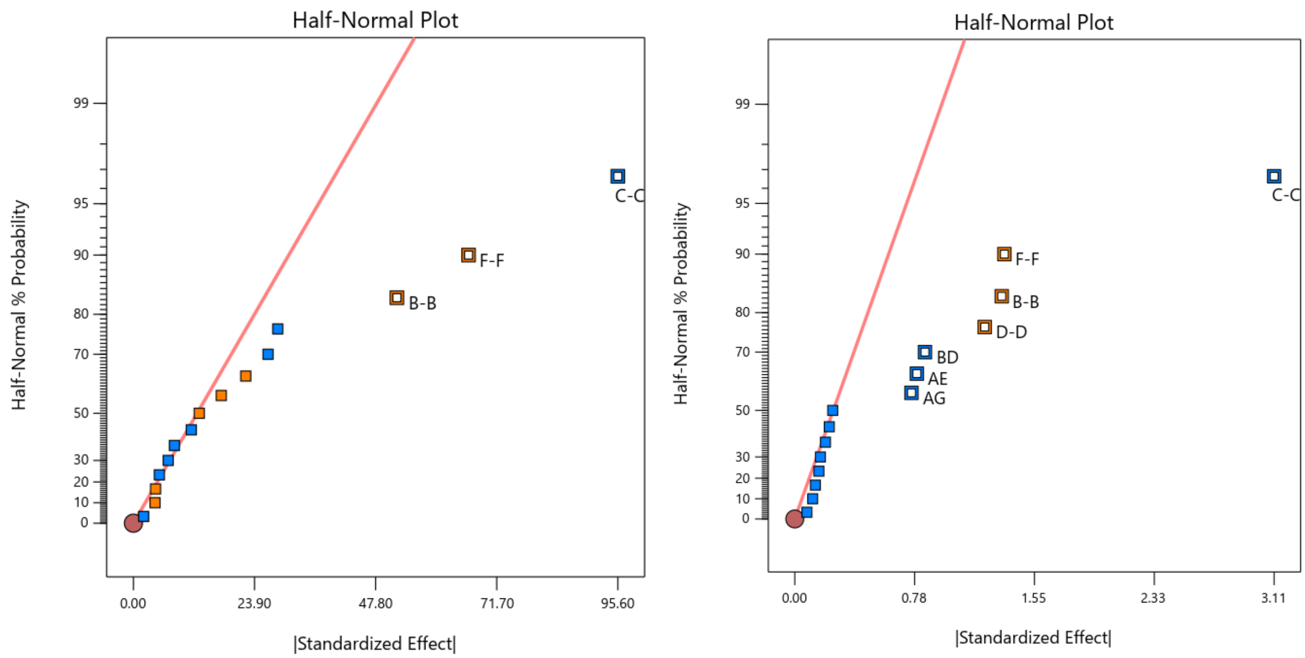

(a) *(b)*

Figure 9. Sensitivity analysis results for the coupling beams' initial yielding: (a) half-normal probability plot for the displacement, (b) half-normal probability plot for the sequence.

Coupling beams' initial plastic hinge

Coupling beams' initial plastic hinge formation is affected mainly by the length of the wall (C) (negative effects) and the ratio of the coupling beams' thickness to the walls' thickness (B) (positive effects), with 29.4% and 18.9% contribution percentages. Further, the walls' steel faceplate thickness (E) (negative effects) and interactions between factors A and E (AE) (negative effects), and A and B (AB) (positive effects), with contribution percentages of 8.4%, 7.8%, and 7.6%, respectively, are influential (Fig. 10).

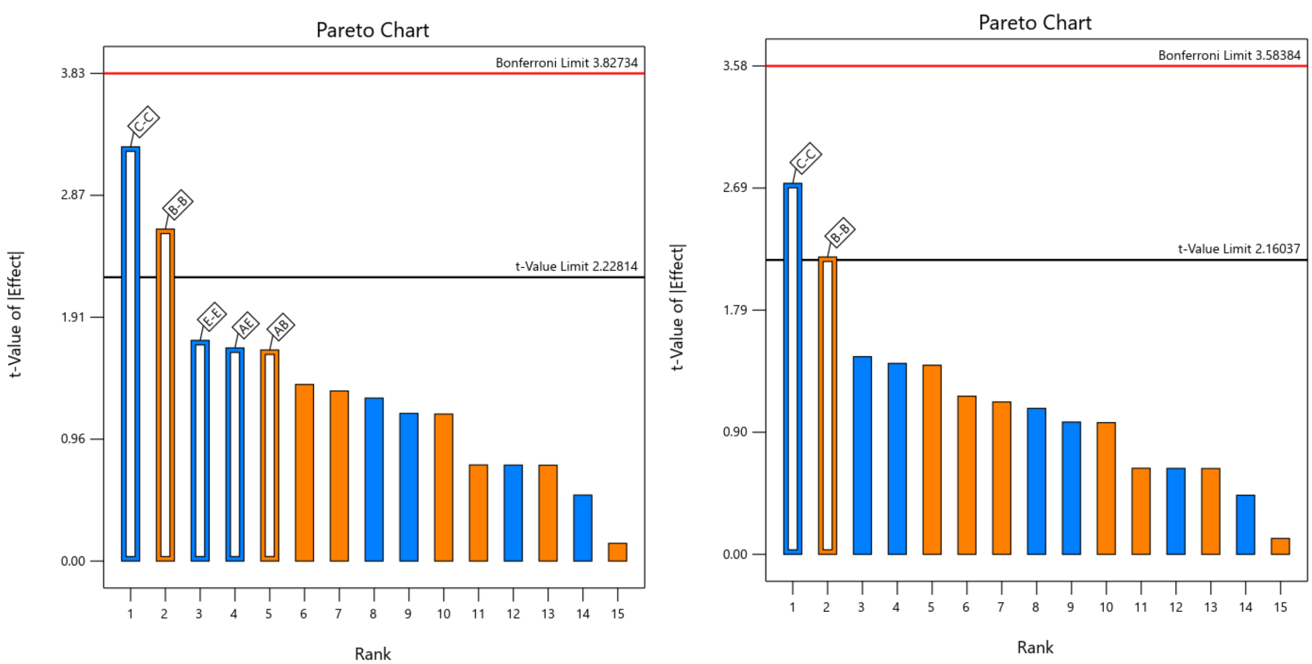

(a) *(b)*

Figure 10. Sensitivity analysis results for the coupling beams' initial plastic hinge: (a) Pareto chart for displacement, (b) Pareto chart for the sequence.

Coupling beams' last plastic hinge

Fig. 11 shows the half-normal probability plot for the coupling beams' last plastic hinge in terms of the displacement and order of occurrence for different factors. Based on displacement and sequence, the ratio of the coupling beams' thickness to the walls' thickness (B) is the most influential factor in the responses, with 24.5% and 23.2% contribution percentages. According to the displacement at which the last coupling beam occurs, the total thickness of the wall (D), concrete compressive strength (G), and steel yield strength (F) are also critical, with contribution percentages of 15.5%, 12.9%, and 11.0%. Steel yield strength (F) and the total thickness of the wall (D) are two other significant factors, according to the sequence, with 14.12% and 13.9% contribution, followed by factors C and G. It can be concluded that many of the factors can influence the occurrence of the last plastic hinge. B, D, and F positively affect the responses, while G has adverse effects.

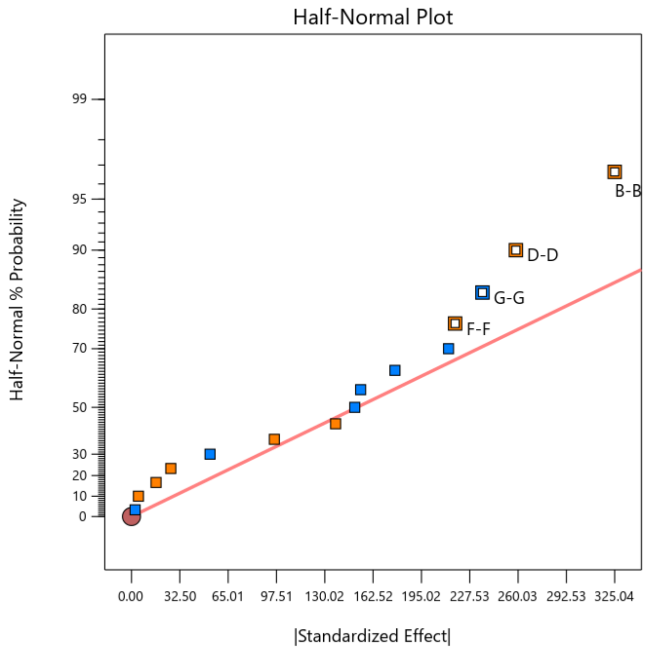

(a)

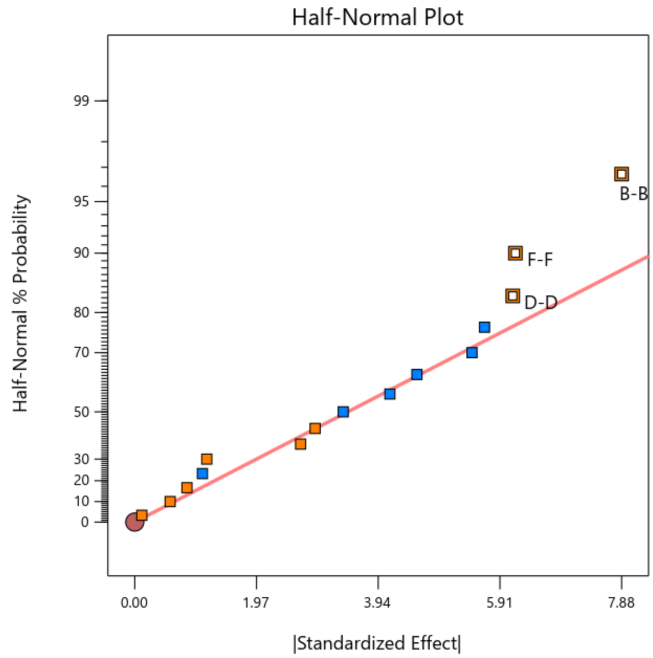

(b)

Figure 11. Sensitivity analysis results for the coupling beams' last plastic hinge: (a) half-normal probability plot for displacement, (b) half-normal probability plot for the sequence.

Walls' initial yielding

The Pareto charts for the walls' initial yielding based on the displacement and sequence are shown in Fig. 12. The length of the wall (C), steel yield strength (F), the walls' steel faceplate thickness (E), and the ratio of the coupling beams' thickness to the walls' thickness (B) are the most influential factors. However, the order of importance of these effects depends on whether the displacement or sequence of occurrences is monitored. For instance, from a displacement point of view, the length of the wall (C), with a 27.0% contribution percentage, is the most significant factor. On the other hand, the walls' steel faceplate thickness (E), with 34.5%, is the most influential factor, based on the sequence of initial yielding occurrence. Among factors, C and B have negative effects on the initial yielding occurrence, while F and E have positive effects.

Maximum base shear

Results show that the length of the wall (C) with positive effects is the most influential factor on the maximum base shear, with a 61.3% contribution percentage. According to the results of displacement and the time at which the system achieves its maximum base shear (Fig. 13), four factors of the ratio of the coupling beams' thickness to the walls' thickness and the total thickness of the wall interaction (BD), walls length (C), the interaction between factors A, B, and D (ABD), and the coupling beams aspect ratio (A) are the most significant. Fig. 14 shows the plots for BD interactions. In Fig. 14a, two low (−) and high (+) levels are selected for D, and the displacement at which the maximum base shear occurs is monitored based on the change in B varies from 0.6 to 1. For a low level of D, the displacement at which the maximum base shear occurs increases with an increase in B. However, factor B adversely affects the results when a high level of D is selected. Fig. 14b shows the 3D surface plot.

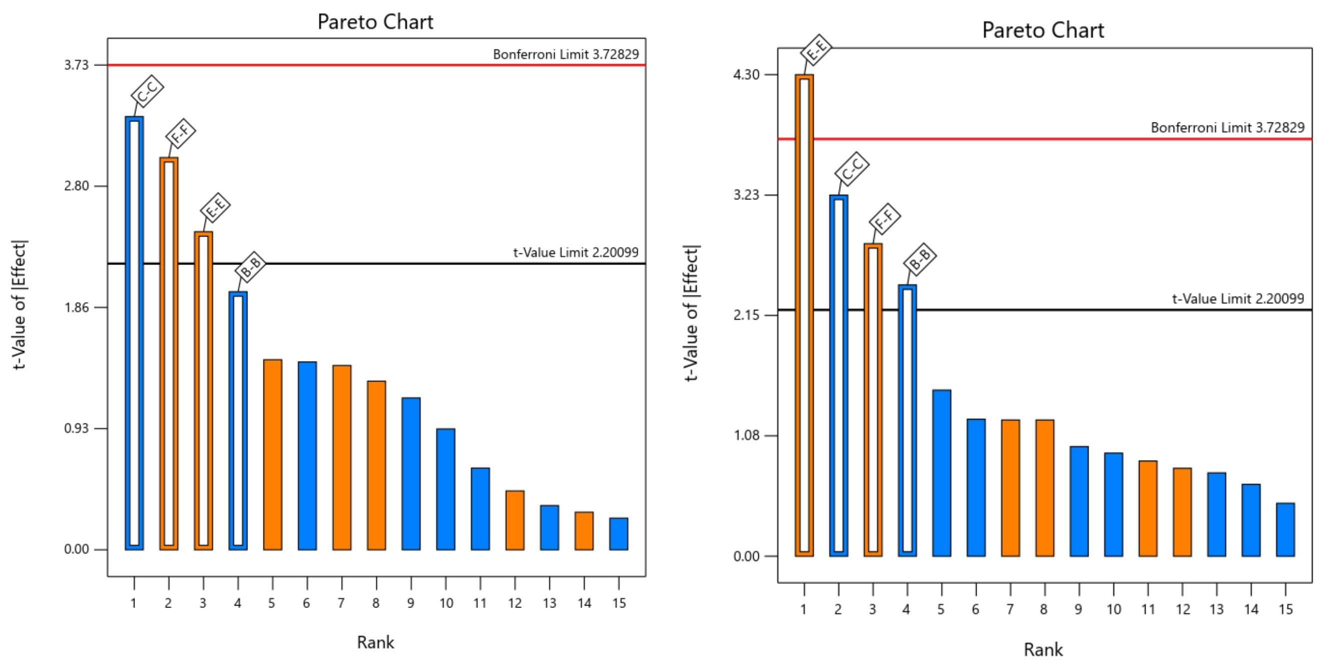

(a) *(b)*

Figure 12. Sensitivity analysis results for the Walls' initial yielding: (a) Pareto chart for displacement, (b) Pareto chart for the time.

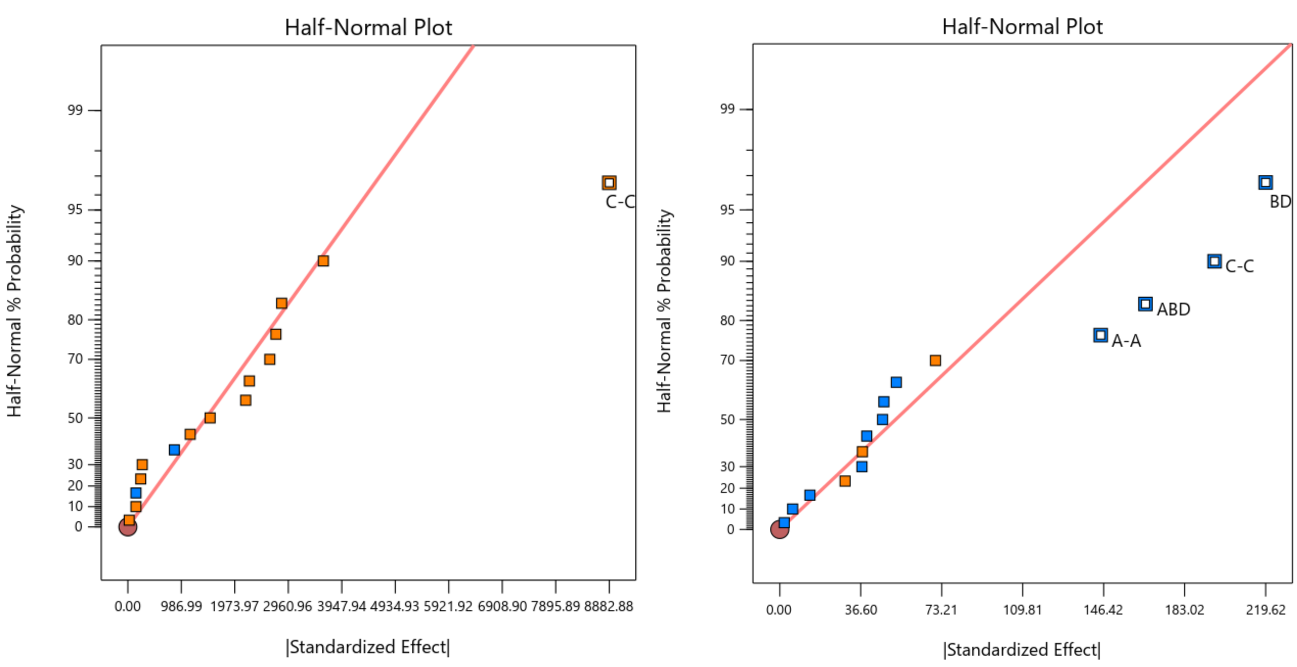

(a) *(b)*

Figure 13. Half-normal probability plot for the maximum base shear: (a) maximum base shear value, (b) maximum base shear displacement.

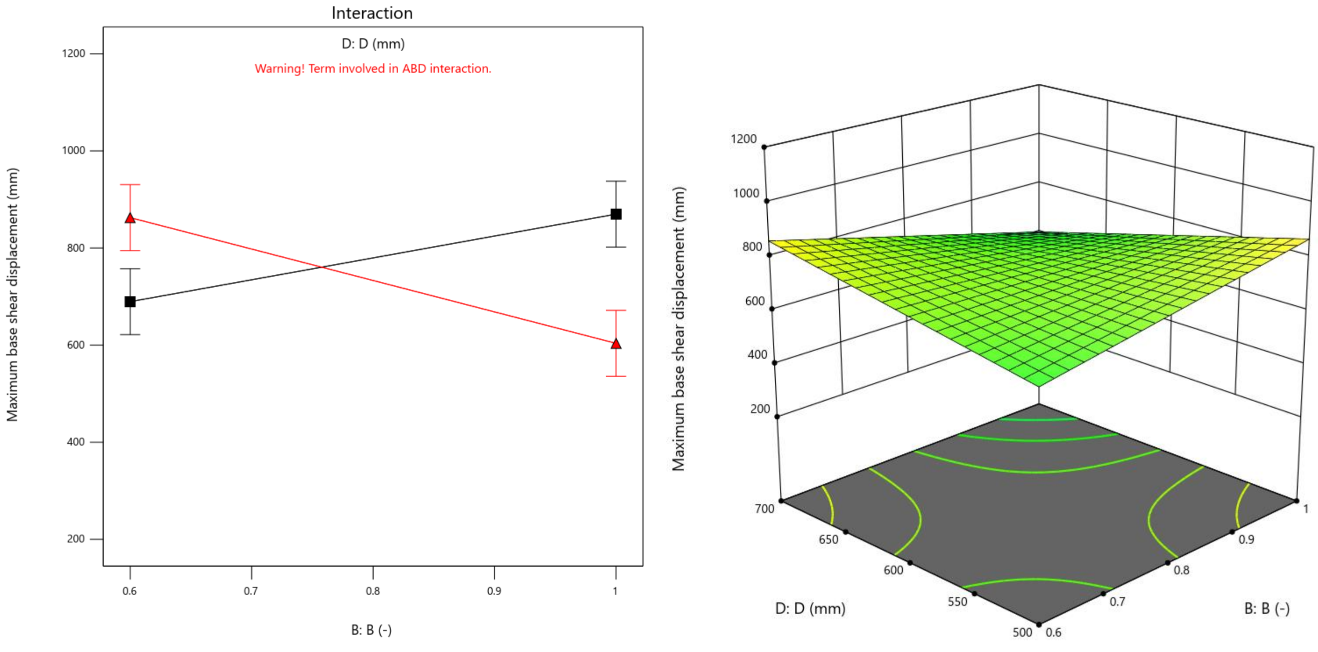

(a) *(b)*

Figure 14. Interaction between factors B and D for the maximum base shear displacement: (a) interaction plot, (b) 3D surface plot.

CONCLUSIONS

This study conducted a sensitivity analysis on the CC-PSW/CF, considering seven design factors and 12 responses. Statistical tools are utilized to determine the most influential factors on each response and any possible factor interactions. The main results are summarized below:

1. The most significant factor in the initial stiffness of the system is the length of the wall, with an 81.0% contribution percentage. This factor positively affects the initial stiffness of the CC-PSW/CF.
2. Three factors of the length of the wall (factor C), steel yield strength (F), and The ratio of the coupling beams' thickness to the walls' thickness (B) are more influential than other factors on the coupling beams' initial yielding.
3. The length of the wall (C) and the ratio of the coupling beams' thickness to the walls' thickness (B), with 29.4% and 18.9% contribution percentages, are the most significant factors affecting the initial plastic hinges in coupling beams.
4. The ratio of the coupling beams' thickness to the walls' thickness (B), steel yield strength (F), and the total thickness of the wall (D) are the most significant factors influencing the coupling beams' last plastic hinge formation.
5. From a displacement point of view, the length of the wall (C), with a 27.0% contribution percentage, and from a time and sequence point of view, the walls' steel faceplate thickness (E), with 34.5%, are the most influential factors on the walls' initial yielding.
6. The length of the wall (C) is the most significant factor influencing the maximum base shear values, with a 61.3% contribution percentage. The ratio of the coupling beams' thickness to the walls' thickness and the total thickness of the wall interaction (BD) is the most significant factors in the displacement and time of the maximum base shear occurrence.

ACKNOWLEDGMENTS

The financial support from the Canadian Institute of Steel Construction **(**CISC**)** and the Natural Sciences and Engineering Research Council of Canada (NSERC) through the Discovery Grant is gratefully acknowledged.

REFERENCES

[1] Broberg, M., Shafaei, S., Kizilarslan, E., Seo, J., Varma, A. H., Bruneau, M., and Klemencic, R. (2022). "Capacity design of coupled composite plate shear wall–concrete-filled system". *Journal of Structural Engineering*, 148(4), 04022022.

[2] American Society of Civil Engineers - ASCE (2016). *ASCE/SEI 7-16*: Minimum Design Loads and Associated Criteria for Buildings and Other Structures.

[3] American Society of Civil Engineers - ASCE (2022). *ASCE/SEI 7-22*: Minimum Design Loads and Associated Criteria for Buildings and Other Structures.

[4] Ji, X., Cheng, X., Jia, X., and Varma, A. H. (2017). "Cyclic in-plane shear behavior of double-skin composite walls in high-rise buildings". *Journal of Structural Engineering*, 143(6), 04017025.

[5] Shafaei, S., Varma, A. H., Seo, J., and Klemencic, R. (2021). "Cyclic lateral loading behavior of composite plate shear walls/concrete filled". *Journal of Structural Engineering*, 147(10), 04021145.

[6] Seo, J., Varma, A. H., Sener, K., and Ayhan, D. (2016). "Steel-plate composite (SC) walls: In-plane shear behavior, database, and design". *Journal of Constructional Steel Research*, 119, 202-215.

[7] Kenarangi, H., Kizilarslan, E., and Bruneau, M. (2021). "Cyclic behavior of c-shaped composite plate shear walls–Concrete filled". *Engineering Structures*, 226, 111306.

[8] Kizilarslan, E., Broberg, M., Shafaei, S., Varma, A. H., and Bruneau, M. (2021). "Non-linear analysis models for composite plate shear walls-concrete filled (C-PSW/CF)". *Journal of Constructional Steel Research*, *184*, 106803.

[9] Shafaei, S., Varma, A. H., Broberg, M., and Klemencic, R. (2021). "Modeling the cyclic behavior of composite plate shear walls/concrete filled (C-PSW/CF)". *Journal of Constructional Steel Research*, 184, 106810.

[10] Kizilarslan, E., Broberg, M., Shafaei, S., Varma, A. H., and Bruneau, M. (2021). "Seismic design coefficients and factors for coupled composite plate shear walls/concrete filled (CC-PSW/CF)". *Engineering Structures*, 244, 112766.

[11] Broberg, M. R., Shafaei, S., Seo, J., Varma, A. H., and Agrawal, S. (2019). "Introduction to seismic analysis of coupled composite plate shear walls-concrete-filled (CC-PSW/CF)". In *SSRC Conferences*, April (pp. 2-5).

[12] ABAQUS. (2021). ABAQUS/Standard and ABAQUS/Explicit – Version 2021. ABAQUS Theory Manual, Dassault System.

[13] Bruneau, M., Varma, A. H., Kizilarslan, E., Broberg, M. R., Shafaei, S., and Seo, J. (2019). "R-factors for coupled composite plate shear walls/concrete filled (CC-PSW/CF)". *Charles Pankow Foundation & American Institute of Steel Construction*.

[14] DX9. Design-Expert® software version 9; 2013.

[15] Mohammadi Nia, M., and Moradi, S. (2020). "Limit state behavior and response sensitivity analysis of endplate steel connections with shape memory alloy bolts". *Journal of Intelligent Material Systems and Structures*, 31(18), 2071-2087.

[16] Eom, T. S., Park, H. G., Lee, C. H., Kim, J. H., and Chang, I. H. (2009). "Behavior of double skin composite wall subjected to in-plane cyclic loading". *Journal of Structural Engineering*, 135(10), 1239-1249.